Electronic Letters on Computer Vision and Image Analysis 20(2):38-50;2021

Underwater Acoustic Image Denoising Using Stationary Wavelet Transform and Various Shrinkage Functions

R. Priyadharsini[1], T. SreeSharmila[2]

1. Associate Professor, Department of CSE, SSN College of Engineering
2. Associate Professor, Department of IT, SSN College of Engineering

Received 2nd of December 2020; accepted 22nd of July 2021

Abstract

Underwater acoustic images are captured by sonar technology which uses sound as a source. The noise in the acoustic images may occur only during acquisition. These noises may be multiplicative in nature and cause serious effects on the images affecting their visual quality. Generally image denoising techniques that remove the noise from the images can use linear and non-linear filters. In this paper, wavelet based denoising method is used to reduce the noise from the images. The image is decomposed using Stationary Wavelet Transform (SWT) into low and high frequency components. The various shrinkage functions such as Visushrink and Sureshrink are used for selecting the threshold to remove the undesirable signals in the low frequency component. The high frequency components such as edges and corners are retained. Then the inverse SWT is used for reconstruction of denoised image by combining the modified low frequency components with the high frequency components. The performance measure Peak Signal to Noise Ratio (PSNR) is obtained for various wavelets such as Haar, Daubechies, Coiflet and by changing the thresholding methods.

Keywords: Acoustic images, Coiflet, Daubachies, Haar, Stationary Wavelet, Sureshrink, Visushrink

1 Introduction

Maritime archaeology is the study of the undersea environment which involves surveying the sea bed for detection of living and non-living resources. This type of study is possible only with sonar systems. As light attenuates in shorter distance inside water, sound is used to produce signals and to convert that into 2D images. Sonar is a powerful tool for surveying the sea floor. The sonar array emits fan shaped sound signals perpendicular to the direction of the travel of the device. The backscattered signals [3] from each ping on the port will be used to produce the image on the top processing unit. The sonar transmits high frequency sound pulses to travel in the water medium and hits the objects. The reflected waves are relayed to the software which converts the return pulses into images. Based on the distance of the object and strength of the echoes, the images are formed. Image denoising, a preprocessing step in image processing plays an important role for image enhancement, image segmentation and object recognition. Noise in generic images may occur during

Correspondence to: priyadharsinir@ssn.edu.in
Recommended for acceptance by Angel D. Sappa
https://doi.org/10.5565/rev/elcvia.1360
ELCVIA ISSN: 1577-5097
Published by Computer Vision Center / Universitat Autonoma de Barcelona, Barcelona, Spain

acquisition, transmission and storage. The acoustic images are affected by speckle noise which is a multiplicative noise [4]. The noises in the image can be removed by filtering methods in the spatial domain. A wavelet based denoising method has been proved to be better for texture images [33].

The remainder of this paper is organized as follows. In section II, the related work in denoising is discussed. Wavelet based denoising process is explained in section III. In section IV, Stationary Wavelet Transform along with all wavelet families such as Haar, Daubechies and Coiflet are discussed. In section V, shrinkage denoising functions are elaborated. In section VI, experimental results with performance measures are demonstrated. Finally, the conclusion part is discussed in section VII.

2 Related work

Image denoising is one of the preprocessing techniques aimed at removing the noise from the image. This technique aims at denoising all types such as satellite images, medical images, thermal images, generic images, etc. to improve the quality of the images. The literature survey has proved that the images are corrupted by noise during acquisition and transmission. The satellite images were denoised using hybrid directional lifting [1] technique to retain the details of the images. A framework [2] for nonlinear, adaptive smoothing, bilateral filtering and mean shift were attempted to smooth the images in many iterations. Several methods have been proposed to denoise the images in the wavelet domain by improving the shrinkage techniques by using suboptimal universal threshold [7] and same window size in all wavelet bands. A locally adaptive patch based thresholding [8] was also used for replacing the standard thresholding technique. In a work proposed for hyperspectral image denoising [9][10], before applying the SURE method for thresholding, first order roughness penalty was used to exploit the multiresolution property of the wavelet. The principal component analysis was also used to decorrelate the image from the noise.

As the wavelet transform is an effective multiscale and multidirection analysis tool, a non subsampled shearlet transform [11][12], dual tree complex wavelet transform [15] and Contourlet transform [27] were used to decompose the image and then a wiener filter and an adaptive bayesian threshold were used to denoise the image. An interscale orthonormal wavelet thresholding [13] [26] algorithm was introduced to improve the SURE approach. Both in spatial and frequency domain the web images were denoised and wavelet based image fusion methods [14] have been introduced. The filtering techniques such as Anisotropic Diffusion filter, Wiener filter, Non-Local Means [17][18][30], Bilateral filters were used for denoising the Chinese calligraphy images and a parallel non local means filtering [20] used for medical images. An adaptive data driven threshold using bayesian framework [19] in wavelet soft thresholding were used both for image denoising and compression. In diffusion based methods [21], the image is divided into regions where the gradient is lower than, between and higher than the smoothing threshold. All the denoising methods aim at removing the noise without disturbing the edges.

A local linear kernel smoothing [25], in which local pixels in the neighborhoods were used to differentiate the smooth areas and the edge pixels have been proposed. A Perona–Malik (MPM) model based on directional Laplacian [22] was used for denoising the noise by preserving the edges and block matching - 3D filtering [24] method that uses fixed directions to search for the edges are proposed. Machine learning techniques such as fuzzy C-mean clustering were employed to despeckle the edge-removed Satellite image [28]. In directionlet domain [29], image denoising with multidirectional shrinkage functions were used to remove the noise and for preserving the edges. During the data collection of acoustic signals, the non-stationary background noises are unavoidable. In order to suppress the noise interference in the underwater acoustic signals, a convolutional denoising autoencoder [31] was designed to train the segmented multi-images in parallel to acquire denoising features using Random forest classification. For improving the classification accuracy, the weight fusion is used to initialize parallel classifier. Similarly noise reduction technique for underwater acoustic signals was proposed using ensemble methods. The technique [32] adopts Complete Ensemble Empirical Mode Decomposition with Adaptive Noise (CEEMDAN), Minimum Mean Square Variance Criterion (MMSVC) and Least Mean Square Adaptive Filter (LMSAF). These methods could suppress mode mixing, identify noisy intrinsic mode function and overcome the selection of decomposition number and basis function for wavelet noise reduction. From these existing methods, it is evident that acoustic images need a denoising process. There are many filtering techniques that remove the noise in the images. Since the acoustic images are low resolution images, these filtering techniques tend to smooth the images and strong edges are removed. The objective of this work is to smooth the images to remove the noise by preserving the edges.

3 Wavelet based Denoising process

Speckle noise is a multiplicative granular noise caused due to random fluctuations in the return acoustic signal. It affects the image as it is from multiple distributed targets. In acoustic bearing displays, the signals form continuous tracks and noise often takes isolated speckle. These affected images should be either smoothed or denoised for removing the noise. Smoothing is entirely different from denoising as it suppresses high frequency components such as edges and retains low frequency elements. On the other hand, denoising removes noise regardless of the frequency content of the signal. Among the denoising techniques available, wavelet-based denoising methods have been proved to be performing well. The following are the steps involved in wavelet based denoising and depicted in figure 1.

- Decompose the image using SWT
- Apply shrinkage denoising techniques for wavelet coefficients
- Image reconstruction using Inverse SWT

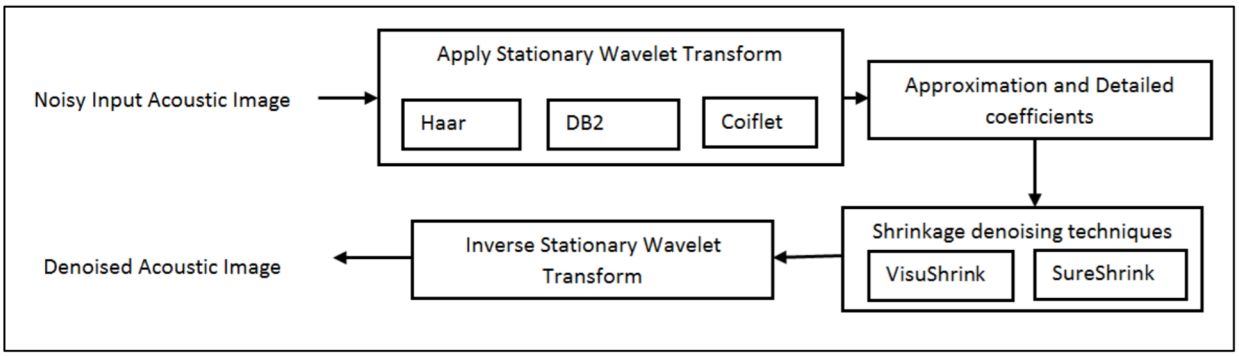

Figure 1: Steps in wavelet based denoising process

4 Stationary Wavelet Transform

The properties such as sparsity and multiresolution structure make wavelet perform well for image denoising [4]. The transients and singularities can be represented as sparse piecewise regular 1D signals using wavelet basis. In 2D images large wavelet coefficients are in the edges and irregular textures. Based on the functionalities, wavelet can be classified as continuous, discrete, stationary, multiwavelet, etc. The continuous wavelet deals only with 1D signals whereas Discrete Wavelet Transform (DWT) is used for 2D images to capture frequency and location information. Even though DWT works well for many image applications, they lack in translation invariant property. The images are decomposed into low frequency and high frequency components using DWT. These components are half the length of the original image. During the analysis phase, the downsamplers along with the filters are used to produce the frequency components and in the synthesis phase, upsamplers are used.

The Stationary wavelet transform (SWT) was designed to overcome the translation invariant property by removing the downsamplers and upsamplers in the DWT. In order to maintain the same length of the image, redundant scheme is used. It is otherwise referred as undecimated wavelet transform. The first step in SWT is to apply high and low pass filters to the image at each level. The resultant components are not decimated. Then the filters are modified at each level by padding zeroes.

The following figure 2a and 2b show how the image is decomposed into low frequency and high frequency sub bands. As shown in figure 2a, during the first level of decomposition, the image is split into four components such as LL (Low Low), LH (Low High), HL (High Low), HH (High High) frequency. LL represents the low frequency smooth areas in an image, LH, HL, HH represents high frequency detailed edge features of an image. Figure 2b represents the second level of decomposition where the LL smooth low frequency component is further divided into four detailed components. The various levels of decomposition help in understanding the details of images in various frequencies.

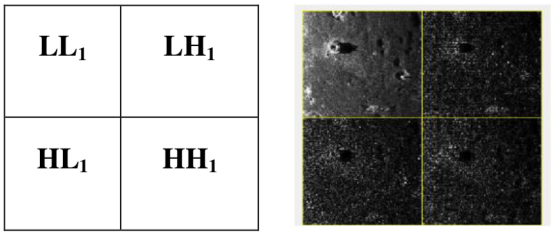

Figure 2a: First level of decomposition

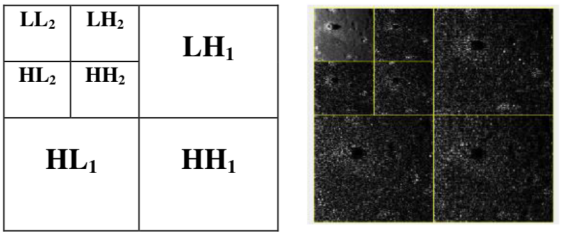

Figure 2b: Second level of decomposition

In this work, three different types of wavelets such as Haar, Daubechies and Coiflet are used for decomposing the acoustic image and their inverse to reconstruct the denoised image.

4.1 Haar Wavelet

A subset $\{v_1,....v_k\}$ of a vector space V with their inner product $\langle v_i,v_j\rangle=0$ is said to be orthonormal when $i\neq j$. Then the vectors are mutually perpendicular and linearly independent. The Haar wavelet [4] is the simplest orthonormal wavelet basis. It is capable of exactly reconstructing the edges without affecting their characteristics. The Haar transform reflects changes only between adjacent pixel pairs and does not have any overlapping windows making the transform very easy to use. It is used to detect sudden changes in pixel intensities. The scaling and wavelet function coefficients, used by this transform calculates pair wise averages and differences. The wavelet function can be represented using Eq(1)

$$\psi(t) = \begin{cases} 1 & 0 < t < {}^1/_2 \\ -1 & {}^1/_2 < t < 1 \\ 0 & otherwise \end{cases} \quad (1)$$

The scaling function is defined in the Eq(2)

$$\varphi(t) = \begin{cases} 1 & 0 \leq t < 1 \\ 0 & otherwise \end{cases} \quad (2)$$

4.2 Daubechies Wavelet

The Haar transform is simple to use and decompose the image but it does not provide required smoothing. To incorporate the required smoothness, Daubechies wavelet family [4] was introduced and characteristics by a maximal number of vanishing moments. It is a popular orthogonal wavelet used for texture feature analysis. The Daubechies wavelet uses overlapping windows and not adjacent pixel values, which makes all changes between pixel intensities to be reflected. The smoothness required for noise removal is achieved as Daubechies averages over more pixels. The Daubechies D4 transform has four wavelet and scaling coefficients. The sum of the scaling function coefficients are also one, thus the calculation is averaging over four adjacent pixels.

4.3 Coiflet Wavelet

Coiflets are similar to Daubechies wavelet except that they use six scaling and wavelet function coefficients [4]. As the number of function coefficients increases the overlapping tends to be high. In turn the pixel averaging and differencing also increases that leads to more smoothing. They perform well for texture image denoising.

5 Thresholding techniques

There are many filtering techniques in the spatial domain both linear and nonlinear used for smoothing the images. These techniques tend to reduce the noise. The degree of blurring and smoothing depends on the size of the kernel being convolved with the image. In wavelet domain, the filter size can be fixed but the image can be viewed in multiresolution. Thresholding, a simple non-linear technique plays a vital role in operating on the wavelet coefficient. The selection of threshold can be done using hard thresholding or soft thresholding.

Hard threshold:

Hard thresholding method follows a strict strategy where either coefficients are retained as such or set to zero. The coefficients obtained using the wavelet transform are compared with the threshold value. If the coefficient is less than or equal to threshold it is set to zero else coefficient is retained. For a given threshold ***T***, Eq(3) represents the hard thresholding,

$$\mathrm{D^H(Co|T)} = \begin{cases} 0 & \text{for } |\mathrm{Co}| \leq T \\ \mathrm{Co} & \text{for } |\mathrm{Co}| > T \end{cases} \tag{3}$$

Soft Threshold:

In case of spatial domain filtering, hard thresholding method can be useful as they work on pixel intensity. But in wavelet domain, the coefficients are used for image denoising, so hard thresholding is not preferred. The soft thresholding, otherwise called as wavelet shrinkage well suits for image denoising in wavelet domain. Here, given the threshold ***T,*** the wavelet coefficient is compared with the T value. If coefficient is less than or equal to ***T*** then set to *0* otherwise perform *(Co-T).*If coefficient is less than **-*T***, then perform *(Co+T).*Eq(4) defines the soft threshold:

$$\mathrm{D^S(Co|T)} = \begin{cases} 0 & \text{for } |\mathrm{Co}| \leq \mathrm{T} \\ \mathrm{Co} - \mathrm{T} & \text{for } \mathrm{Co} > T \\ \mathrm{Co} + \mathrm{T} & \text{for } \mathrm{Co} < -T \end{cases} \tag{4}$$

Shrinkage Denoising techniques:

VisuShrink and SureShrink are the shrinkage denoising techniques used in the selection of thresholds in wavelet domain filtering. The wavelet basis [5] differentiates the image into large coefficients which are the original signals and small coefficients represent the noise. Modifying the coefficients the noise can be removed from the meaningful signal that is part of the image.

VisuShrink: Visually calibrated Adaptive Smoothing

Visushrink is a threshold selection technique proposed by Donoho and Johnstone [6]. The threshold is calculated by the Eq(5)

$$T = \sigma\sqrt{2\log(I)} \tag{5}$$

where ***T*** *- the calculated threshold,* $\boldsymbol{\sigma}$ *- Standard deviation of the noise,* ***I****- Input image*

Based on the input either hard thresholding or soft thresholding techniques are selected. This threshold is called universal threshold as it is derived under the constraint with high probability that estimate should be smooth as the image. The threshold calculated will be high for edge features and very low for noise. Thus, the threshold does not adapt well to discontinuities in the signal. Visushrink procedure guarantees highly smoothed denoised image but the features are not preserved as the threshold is large. It also fails to adapt to the various statistical and structural properties of the wavelet tree. Hard and soft thresholding decides on the degree of smoothing the images. Normally Hard thresholding preserves the edge features by providing less smoothing effect. On the other hand Soft thresholding provides more smoothing results. As acoustic images vary in resolution and quality it is required to select the type of thresholding during denoising process. If the value of the variable *n* is less than 2 then soft thresholding is applied to increase the level of smoothing. If the value is greater than 2 then hard thresholding is applied to preserve the features.

VisuShrink: Visually calibrated Adaptive Smoothing

Procedure:

1. *Calculate the threshold from the image*

$$T = \sigma\sqrt{2\log(I)};$$

where ***T*** *- the calculated threshold,* $\boldsymbol{\sigma}$ *- Standard deviation of the noise,* ***I****- Input image*

2. Call the function hardthresh or Softthresh based on the variable n

```
if (n < 2)
type = 'softthreshold';
x = softthresh(I,T);
else
type = 'hardthreshold';
x = hardthresh(I,T);
```

Function*hardthresh(I,T) // hard threshold function definition*

$if\,(abs(I) > T)$
$x = I;$
$else$
$x = 0;$

Function*softthresh(I,T) // Soft threshold function definition*

$if\,(abs(I) \le T)$
$x = 0;$
$else$
$temp = (abs(I) - T);$
$temp = (temp + abs(temp))/2;$
$x = sign(I) * temp;$

SureShrink: Stein's Unbiased Risk Estimate Shrinkage function

SureShrink follows an adaptive technique for threshold selection. If the image contains more features, the reconstruction will also have preserved features. If the image contains more smooth areas, the reconstructed image will also have more smooth areas. The advantages of the SureShrink are evident when the image has more features on a smooth background. All detailed sub band are extracted from the image using SWT. The sub band sizes are computed and the noisy sub band is filled using zero. Then the threshold vector is produced based on the sorted values of all neighborhoods. The threshold is selected based on the risk which is minimum.

SureShrink: Adaptive Threshold Selection Using Principle of SURE (SURE refers to Stein's Unbiased Risk Estimate)

Procedure:

1. *Calculate the threshold using Surethresh function*

Function *thresh=Surethresh(I) // Surethresh function definition*

$l = length(I);$
$s = sort(abs(I)).\hat{}2;$
$s1 = cumsum(s);$
$risk = (l - (2 * (1:l)) + s1)/l;$
$[guess, best] = \min(risk);$
$thresh = sqrt(s(best));$

2. Call the function Surethresh

Thresh=Surethresh(I);

```
3.Call the function hardthresh

X=hardthresh(I,thresh);
```

6 Experimental results

The acoustic images used for experiment were acquired using Edgetech 4125 Side scan sonar. The sonar was immersed in the sea to a depth of 20 meters and the objects were sensed using the Discover software in the top processing unit. The obtained video files were split into frames and were resized to 512 x 512 Jpeg acoustic images each for processing. The proposed denoising method was implemented using Matlab 9.5 Release R2018b.

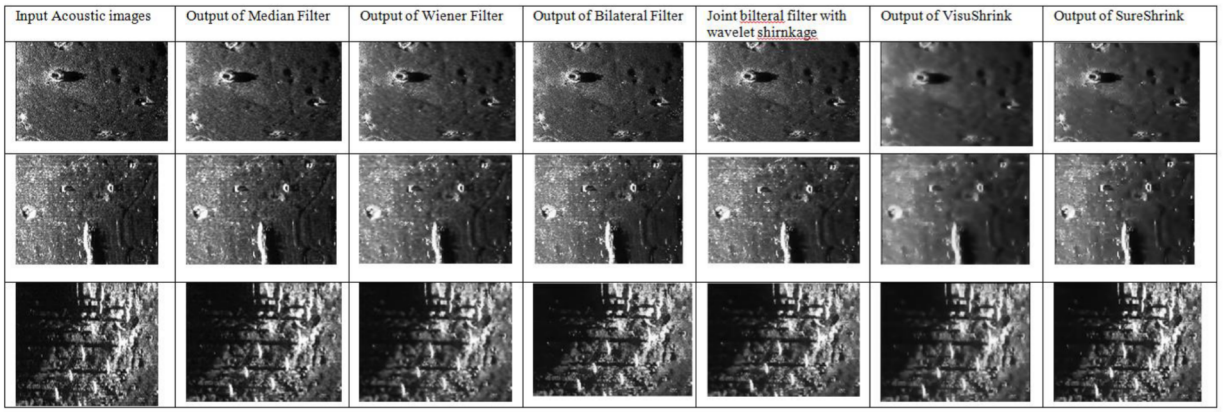

Figure 3: Results of acoustic images denoised using various filtering techniques

The experimental results in Figure 3 and objective measures in table 1 shows that median, wiener, bilateral and Joint bilteral filter with wavelet shirnkage filters in the spatial domain did not denoise the acoustic image to an extent. But decomposing the image using SWT and applying the Shrinkage techniques such as Visushrink and Sureshrink leads to good denoising of acoustic images. The denoising step is considered as the preprocessing step in the object detection phase. In acoustic images, the seafloor and sediments are dominant compared to the object. The results of Visushrink and Sureshrink has denoised the image such a way that seafloor and sediments are smoothed while preserving the objects and their features.

6.1 Performance measure

For comparison, objective measures such as Peak Signal to Noise Ratio (PSNR), Speckle Image Statistical Analysis (SISA) and Feature Preserving Index (FPI) [23] are used to evaluate the performances of the system. The PSNR is the ratio of the maximum power and the noise power, which is defined by,

$$PSNR = 10\log_{10}\frac{255^2}{MSE} \qquad (10)$$

Where $$MSE = \frac{\sum_{M,N}[c(x,y) - f(x,y)]^2}{MxN} \quad (11)$$

MSE is the mean square error between the reconstructed image $c(x, y)$ and the original image $f(x, y)$ where M and N are the sizes of row and column respectively.

The ratio of the original image and the filtered image is actually an image that represents the amplitude of the speckle:

$$SP = \frac{R}{R_f} \quad (12)$$

Where SP is the resulting speckle image R is the original image and R_f is the filtered image [34]. Statistics, such as its mean and standard deviation, can be computed for this ratio or speckle image. Ideally, the histogram of the speckle image would have a normal distribution with a mean around 1.0. The mean of the speckle image is a good indicator of a filter's ability to retain an image's original mean values. the closer the mean is to 1.0, the better is the filter's ability in retaining image content.

The feature-preserving index is a measure for assessing a filter's ability to preserve linear features and subtle structure. For a one-pixel wide linear feature of n-pixel length, the FPI is given by

$$FPI = \frac{\sum_1^n (2.R_f - R_{f1} - R_{f2})}{\sum_1^n (2.R - R_1 - R_2)} \quad (13)$$

where R is the original value of a pixel on the linear feature, R_1 and R_2 are the neighbouring pixels on both side of the feature, and R_f, R_{f1}, and R_{f2} are the filtered values of the corresponding pixels. Increase in the FPI values show the more features being preserved.

The following tables 1,2,3 show the PSNR, SISA, FPI values for the techniques median, wiener, bilateral, joint bilateral filters, SWT denoising using Visushrink and Sureshrink.

	PSNR Values					
Acoustic Images	Median	Weiner	Bilateral	Joint bilteral filter with wavelet shirnkage	Visushrink	Sureshrink
Image 1	17.5749	22.3614	24.5316	27.3409	29.6916	29.9626
Image 2	16.4605	39.8702	25.8564	29.1260	32.8119	33.3823
Image 3	18.6283	27.8548	26.1212	29.9622	32.8679	40.6226
Image 4	17.4652	27.1773	24.2532	28.5661	39.8814	39.5836
Image 5	18.6810	27.7872	29.8511	31.6595	39.3198	40.6803
Image 6	18.8871	24.2978	27.5447	33.2245	38.9237	38.9137
Image 7	16.9008	23.0289	28.1602	34.8964	32.6737	35.1345
Image 8	20.7907	39.8698	27.3463	33.6702	34.0751	35.8462

Table 1: PSNR values for the various techniques

	SISA Values					
Acoustic Images	Median	Weiner	Bilateral	Joint Bilateral Filter with wavelet shirnkage	Visushrink	Sureshrink

Image 1	0.9812	0.9647	0.9647	0.9545	0.9745	0.9876
Image 2	0.9811	0.9894	0.9894	0.9827	0.9926	0.9928
Image 3	0.9778	0.9871	0.9871	0.9688	0.9654	0.9891
Image 4	0.9846	0.9857	0.9857	0.9750	0.8124	0.9871
Image 5	0.9632	0.9816	0.9863	0.9509	0.8457	0.9863
Image 6	0.9619	0.9632	0.9632	0.9627	0.9172	0.9852
Image 7	0.8823	0.9634	0.9634	0.9567	0.8416	0.9817
Image 8	0.8953	0.9698	0.9698	0.9655	0.9214	0.9854

Table 2: SISA values for the various techniques

	FPI Values					
Acoustic Images	Median	Weiner	Bilateral	Joint Bilateral Filter with wavelet shirnkage	Visushrink	Sureshrink
Image 1	0.6186	0.4397	0.6346	0.6214	0.6636	0.8917
Image 2	0.5099	0.4019	0.5586	0.5925	0.6281	0.7280
Image 3	0.4256	0.3890	0.5180	0.7594	0.8354	0.9441
Image 4	0.3139	0.4685	0.4189	0.2352	0.6422	0.8050
Image 5	0.5155	0.6396	0.2754	0.0672	0.8161	0.9622
Image 6	0.4212	0.4277	0.2691	0.6274	0.6943	0.8183
Image 7	0.3402	0.4989	0.1268	0.3865	0.7765	0.8119
Image 8	0.1618	0.6348	0.3587	1.0442	0.7280	0.8417

Table 3: FPI values for the various techniques

The low resolution acoustic images which suffer from speckle noise are denoised using various filtering techniques. The state of art filtering techniques such as median filter, weiner filter and Bilateral filters are applied to suppress the noise. These techniques tend to smooth the images but don't preserve the edges. The PSNR, SISA, FPI values also show that these filtering techniques provide poor performance. Since Wavelet based techniques work on multiresolution based approaches where the details will be preserved in each decomposition, Visushrink and Sureshrink approaches were proposed. The visual results prove that shrinkage based wavelet methods smooth the images to remove the noise still preserving the edges.

Conclusion

This paper aims at denosing the acoustic images in the wavelet domain with shrinkage functions. The characteristics of the acoustic image are very unique that spatial domain filters may not give high quality output during denoising process. The wavelet domain has been proved to be successful for acoustic image denoising. The acoustic images are decomposed using Stationary Wavelet Transform (SWT) to obtain low and high frequency components. Then for removing the noise, the shrinkage functions Visushrink and Sureshrink are applied to the high level coefficients. The acoustic images normally contain textures of seafloor, sediments and underwater objects. It is proved that the Sureshrink technique preserved the edges along the objects and the seafloor and sediments are smoothed. The increased values of PSNR, SISA and FPI also shows that the Sureshrink technique denoises the acoustic images well compared to the other filtering techniques.

Acknowledgement

We would like to thank SSN Institutions for providing financial support to carry out this work successfully.

References

[1] Sree Sharmila Thangaswamy, RamarKadarkarai, Sree Renga Raja Thangaswamy, "Developing an efficient technique for satellite image denoising and resolution enhancement for improving classification accuracy" Journal of Electronic Imaging 22(1), 013013 (23 January 2013).http://dx.doi.org/10.1117/1.JEI.22.1.013013.

[2] D. Barash and D. Comaniciu, "A common framework for nonliear diffusion, adaptive smoothing, bilateral filtering and mean shift" Image and Vision Computing, vol. 22, no. 1, pp. 73–81, January 2004.

[3] Dura E (2011) "Image processing techniques for the detection and classification of manmade objects in side scan sonar images" sonar systems. In: Nikolai K (ed) INTECH.

[4] Gonzalez RC, Woods RE (2007) "Image processing. In: Digital image processing" Prentice Hall, New Jersey, pp. 104–168

[5] Imola K. Fodor, ChandrikaKamath, "Denoising through wavelet shrinkage: An empirical study", Center for applied science computing Lawrence Livermore National Laboratory, July 27, 2001.

[6] David L. Donoho. "Denoising via soft thresholding". IEEE Transactions on Information Theory, 41:613–627, May 1995.

[7] Zhou Dengwen, Cheng Wengang, "Image denoising with an optimal threshold and neighbouring window" Pattern Recognition Letters, vol.29, no.11, pp.1694¨C1697, 2008.

[8] P. Jain , V. Tyagi , "Lapb: locally adaptive patch-based wavelet domain edge-preserving image denoising", Inf. Sci. (Ny) 294 (2015) 164–181 .

[9] B. Rasti , J.R. Sveinsson , M.O. Ulfarsson , J.A. Benediktsson , "Hyperspectral image denoising using first order spectral roughness penalty in wavelet do main", IEEE J. Sel. Top. Appl. Earth Obs. Remote Sens. 7 (6) (2014) 2458–2467.

[10] G. Chen , S.-E. Qian ,"Denoising of hyperspectral imagery using principal component analysis and wavelet shrinkage", IEEE Trans. Geosci. Remote Sens. 49 (3) (2011) 973–980 .

[11] Zhang, Xiaobo. "Image denoising using local Wiener filter and its method noise."*Optik-International Journal for Light and Electron Optics* 127.17 (2016): 6821-6828.

[12] Y. Wang, Y.C. Liu, C.J. Wu, N. Zhang, H.Y. Yang, "An edge-preserving adaptive image denoising", Multimedia Tools Appl. 74 (2015) 11703–11720.\

[13] F. Luisier, T. Blu, M. Unser, "A new SURE approach to image denoising: inter-scale orthonormal wavelet thresholding", IEEE Trans. Image Process. 16(2007) 593–606.

[14] H. Yue, X. Sun, J. Yang, and F. Wu, "CID: Combined image denoising in spatial and frequency domains using Web images," in *Proc. CVPR*,June 2014, pp. 2933–2940.

[15] W. Selesnick, R.G. Baraniuk, N.C. Kingsbury, "The dual-tree complex wavelet transform", IEEE Signal Process. Mag. 22 (2005) 123–152.

[16] Huang, Zhi-Kai, et al. "Comparison of different image denoising algorithms for Chinese calligraphy images." N*eurocomputing* 188 (2016): 102-112.

[17] A.Buades, B.Coll, J.M.Morel, "A non-local algorithm for image denoising", in: Proceedings of IEEE Computer Society Conference on Computer Vision and Pattern Recognition, CVPR2005, IEEE, 2, 2005,pp.60–65.

[18] A.Buades, B.Coll, J.M.Morel, "A review of image denoising algorithms, with a new one", Multiscale Model.Simul.4(2)(2005)490–530.

[19] S. Grace Chang, BinYu, Martin Vetterli, "Adaptive wavelet thresholding for image denoising and compression", IEEE Trans. Image Process.9(9)(2000) 1532–1546.

[20] Mingliang, Xu, et al. "Medical image denoising by parallel non-local means." N*eurocomputing* 195 (2016): 117-122.

[21] Rafsanjani, HosseinKhodabakhshi, Mohammad HosseinSedaaghi, and SaeidSaryazdi. "Efficient diffusion coefficient for image denoising."*Computers & Mathematics with Applications* 72.4 (2016): 893-903.

[22] Y. Wang, J. Guo, W. Chen, W. Zhang, “Image denoising using modified Perona–Malik model based on directional Laplacian”, Signal Process. 93 (2013) 2548–2558.

[23] Z. Wang, A.C. Bovik, H.R. Sheikh, E.P. Simoncelli, “Image quality assessment: from error visibility to structural similarity”, IEEE Trans. Image Process. 13 (2004) 600–612.

[24] Liu, Jing, et al. "Image denoising searching similar blocks along edge directions." *Signal Processing: Image Communication* 57 (2017): 33-45.

[25] I. Gijbels, A. Lambert, P. Qiu, “Edge-preserving image denoising and estimation of discontinuous surfaces”, IEEE Trans. Pattern Anal. Mach. Intell. 28 (7) (2006) 1075–1087.

[26] A. Fathi, A.R. Naghsh-Nilchi, “Efficient image denoising method based on a new adaptive wavelet packet thresholding function”, IEEE Trans. Image Process. 21 (9) (2012) 3981–3990.

[27] X.H. Shen, K. Wang, Q. Guo “Local thresholding with adaptive window shrinkage in the contourlet domain for image denoising” Sci. China Inf. Sci. 56 (9) (2013) 1–9.

[28] W.G. Zhang, F. Liu, L.C. Jiao, B. Hou, S. Wang, R.H. Shang, “SAR image despeckling using edge detection and feature clustering in bandelet domain”, IEEE Geosci. Remote Sens. Lett. 7 (1) (2010) 131–135.

[29] J. Liu, Y.H. Wang, K.J. Su, W.J. He, “Image denoising with multidirectional shrinkage in directionlet domain”, Signal Processing. 125 (C) (2016) 64–78.

[30] B. Goossens, H. Luong, A. Pizurica, and W. Philips, “An improved non-local denoising algorithm,” in *Proc. Int. Workshop Local Non-LocalApprox. Image Process.*, (2008), p. 143.

[31] Zhou, Xingyue, and Kunde Yang. "A denoising representation framework for underwater acoustic signal recognition", *The Journal of the Acoustical Society of America* 147, no. 4 (2020): EL377-EL383.

[32] Li, Yu-xing, and Long Wang. "A novel noise reduction technique for underwater acoustic signals based on complete ensemble empirical mode decomposition with adaptive noise, minimum mean square variance criterion and least mean square adaptive filter", *Defence Technology* 16, no. 3 (2020): 543-554.

[33] Bnou, Khawla, Said Raghay, and Abdelilah Hakim. "A wavelet denoising approach based on unsupervised learning model." *EURASIP Journal on Advances in Signal Processing* 2020, no. 1 (2020): 1-26.

[34] Qiu, Fang, Judith Berglund, John R. Jensen, Pathik Thakkar, and Dianwei Ren. "Speckle noise reduction in SAR imagery using a local adaptive median filter." *GIScience & Remote Sensing* 41, no. 3 (2004): 244-266.